



VIRTIS-H CALIBRATION

	NAME	FUNCTION	SIGNATURE	DATE
Prepared by	S. JACQUINOD JM REESS F. HENRY	Engineer former Project manager V-H Project manager		
Approved by	S. ERARD	V-H team leader		
Authorized by	F. HENRY	V-H Project manager		



1 Document change record

Issue	Date	Name	#	Paragraph	Description of the modification	Reason of the modification
1.0	02/03/16				Creation of the document (based on VVEx doc)	
2.0	05/03/18	SJ, FH, SE			Global update of the document (restructured)	Description of the new calibration process
2.1	06/03/2018 then 10/10/2018	SE			Clarifications, typos Longer discussion of stray light and inclusion of Fig 2a	Comments from archive review, Oct 2018
2.2	23/10/2019	SE			Added provisional estimate of SNR and inclusion of Fig 2b/2c	Comments from archive review, Sept 2019



Table of contents

1 Document change record 2

2 Scope of the document 5

3 Applicable documents 5

4 Reference documents 5

5 List of acronyms 5

6 Virtis-H instrument 6

6.1 Detector size 6

6.2 Virtis-H pixelmap 6

6.3 Acquisition modes 7

6.3.1 Nominal mode 7

6.3.2 Backup mode 7

6.3.3 Internal calibration mode 7

7 VIRTIS-H data 8

7.1 File formats 8

7.1.1 Raw Nominal qubes 8

7.1.2 Dark current qubes in nominal mode 8

7.1.3 Raw Backup qubes 8

7.1.4 Calibrated qubes 9

7.1.5 Internal calibration sequences 9

7.2 Acquisition sequences 9

7.2.1 Observations and darks patterns 9

7.2.2 Acquisition_id 10

7.3 Filenaming convention 10

8 Radiometric Calibration 11

8.1 Calibration process 11

8.1.1 Nominal and Backup modes 11

8.1.2 Despiking and interpolation of dark spectra 13

8.1.3 Detector odd-even effect correction 13

8.1.4 Stray light correction 13

8.1.5 Division by transfer function and exposure time 13

8.1.6 Conversion to reflectance 14

8.2 Open issues on the calibration 14

8.2.1 Stray light correction in nominal mode 14

8.2.2 Improvement of odd/even effect correction 15

8.2.3 Strabismus 15

8.2.4 Signal to Noise estimate 16

9 Spectral calibration 17

9.1 Principle 17

9.2 The PxLMapL 18

9.3 Accuracy of the spectral calibration process 18

9.4 Channels spectral profiles 20

9.4.1 Definition 20

9.4.2 Spectral profile calculation 21



10 Annexes..... 23

10.1 Derivation of the transfer function..... 23

 10.1.1 STEP 1: ground-based calibration..... 23

 10.1.1.1 Odd/even effect correction.....23

 10.1.1.2 Stray light correction24

 10.1.1.3 Correction of H₂O and CO₂ contamination.....25

 10.1.1.4 Creation of a beta transfer function.....25

 10.1.2 STEP 2: Lutetia as a calibrator..... 26

10.2 Corrupted darks 27

 10.2.1 Description of the problem 27

 10.2.2 Workaround 28



2 Scope of the document

This document describes how the science data of VIRTIS-H are calibrated from raw measurements.

3 Applicable documents

None

4 Reference documents

- RD1 RO-VIR-UM-001: VIRTIS Experiment User Manual, issue 3, July 2003
- RD2 VIR-INA-IC-007: ROSETTA-VIRTIS to Planetary Science Archive Interface Control Document (EAICD)
- RD3 VVX-DLR-NC-002: Non-conformance report: H-PEM shutter synchronization
- RD4 VVX-LES-SW-2264: The VIRTIS PDS/IDL software library

5 List of acronyms

ADU	Arbitrary Digital Units
IAS	Institut d'Astrophysique Spatiale (Orsay, France)
IAPS	Istituto di Astrofisica e Planetologia Spaziali (Roma, Italy)
FM	Flight Model
LESIA	Laboratoire d'Etudes Spatiales et d'Instrumentation en Astrophysique (Observatoire de Paris, Meudon, France)
ME	Main Electronics
PDS	Planetary Data System
SCET	SpaceCraft Elapsed Time
TC	TeleCommand
TM	TeleMetry
TF	Transfer Function



6 Virtis-H instrument

VIRTIS-H is a cross-dispersion spectrometer using 8 orders of a diffraction grating [RD1], [RD2]. The 8 spectral orders are spread over the entire surface detector matrix. Each order covers 432×5 pixels, i.e., 432 spectral channels spread on 5 pixels each. In the spatial dimension, the image of the slit only covers 3 pixels, but we integrate on 5 pixels in order not to lose signal. Thus overall only 15% of the 438×270 pixels matrix surface is used. To reduce the overall data rate and volume, H uses the so-called Pixel Map which gives the exact location of the spectra over the H-IR detector.

6.1 Detector size

The Virtis-H detector is a matrix of 438×270 pixels. During development, subsystem tests of Virtis-H were performed without the ME, and the data obtained are full-frame 2d images of 438×270 pixels.

When operated with the ME, only a window of 432×256 pixels of the detector is processed. The location of this window on the detector is described by the parameters Xwin and Ywin, which remained constant during operations (Table 1).

Detector	Xwin	Ywin
FM	3	7

Table 1: window position on Virtis-H detector

6.2 Virtis-H pixelmap

To locate the illuminated pixels on the detector a pixel map is used. This pixel map is the 8×3 -coefficient table of the 2-degree polynomial function per order that identify the pixels that are illuminated on the detector.

This pixel map has to be checked and redefined from time to time.

The pixel map is defined using the internal calibration sessions. This kind of session is a set of 7 acquisitions, all made with the cover closed.

In this mode, the full frame is read and transferred, in order to identify the pixels illuminated through the spectrometer. For each order, a set of 3 coefficients is computed to best fit a 2-degree polynomial function. The process has to be applied to each order. The Pixel map is created as an ASCII file with the 8×3 -coefficient table. Whenever it changes, the new parameters are uploaded to the ME as a TC. The most recent version is used on board to process data acquired in nominal mode.



The pixel map was regularly checked and proved to change very little after launch. Only the Mars flyby data were acquired with an on-board pixel map differing from the actual one. The Mars flyby data acquired in nominal mode can therefore only be partly recovered and calibrated in flux.

6.3 Acquisition modes

VIRTIS-H has 3 acquisition/transfer modes.

6.3.1 Nominal mode

In nominal mode, the downloaded data are spectra, a set of 432x8 pixels. A spectrum can be defined as a composition of the 8 orders imaged on the H-IR detector; the spectrum is extracted from the two-dimensional detector by using the onboard pixelmap. As H has no spatial resolution the 5 pixels of the slit image are averaged together, thus the final end product in the nominal acquisition mode is a 3456 (or 432x8) pixels spectrum representing the full spectral range of the instrument from 1.88 through 5.03 micron.

6.3.2 Backup mode

The full frame can also be downloaded in Backup mode, which is used to check the state of the detector and possible shifts of the pixel map. In this case all 432x256 pixels are sent. The extraction of the spectra with the pixelmap is thus performed on ground.

6.3.3 Internal calibration mode

A sequence of internal calibration of Virtis-H is operated as follows onboard:

- Slit_spectral_calibration : 3 images (H_Image_Slice) with Cover closed, H-Shutter closed then S-lamp switched on, using functional param. integration time H_INT_SPECT_S
- Telescope_spectral_calibration : 2 images (H_image_slice) with H-shutter closed, then T_lamp switched on, using functional param. integration time H_INT_SPECT_T
- Image_slice_radiometric_calibration : 2 images, one H-shutter closed, then R-lamp switched on, using functional param. integration time H_INT_RADIO
- Spectrum_Radiometric_Calibration : same, using the H_spectrum mode (dark with shutter closed, and then R-lamp on)

The total of an internal calibration is $7 \times H_Image_Slice + 2 \times H_spectrum$. The purpose of the internal calibration is the verification of the pixel map and wavelength pixel map (through telescope spectral calibration), the radiometric evolution of the VIRTIS-H chain (lamps+spectrometer+detector), which can be followed along the mission, and the functionality of the on board spectral reconstruction by comparing the H_spectrum mode to Image_Slice mode on the same radiometric calibration image.



The slit calibration using the S-lamp is redundant with the T-lamp, but provides in addition a check of the integrity of the detector, by illuminating a large part of the detector (by scattered light), to follow the bad pixels evolution.

7 VIRTIS-H data

7.1 File formats

A **qube** is a PDS formatted file that contains data [RD2]. A qube is associated to sideplanes providing extra information, in particular selected housekeeping parameters. It can be read with the IDL library *virtispds* or similar software. The output of this routine is a structure, as described in [RD2] and [RD4].

7.1.1 Raw Nominal qubes

A raw Nominal qube contains raw data acquired in Nominal mode. Relevant fields of the structure are:

- *qube*: 3d integer array containing the data. Dimensions are *spec_dim* x 64 x *n_frame*
 - *spec_dim* is the size of one spectrum, and is equal to 8 orders x 432 pixels = 3456
 - 64 is the number of spectra per frame
 - *n_frame* is the number of frame in the qube

Note: The reason of this grouping is that Virtis-H spectra are compressed and processed onboard by packets of 64 spectra [RD1]

- *suffix*: 3d array containing the housekeeping parameters

7.1.2 Dark current qubes in nominal mode

In nominal acquisition mode, the dark spectra are sent and stored separately. The dark current qube only contains spectra acquired with the shutter closed.

7.1.3 Raw Backup qubes

A raw Backup qube contains raw data acquired in Backup mode. In this mode, the whole effective window of the detector is transmitted. Dimensions are 432 x 256 x *n_acquisition*. The fields of the structure are the same as those of the raw Nominal qube. The dark current data are also contained in the qube in acquisition order.



7.1.4 Calibrated qubes

A calibrated qube (nominal or backup) contains calibrated data. Units are $W/m^2/sr/micron$. Relevant fields of the structure are:

- *qube*: 3d float array containing the data. Dimensions are $3456 \times n_acquisitions$
 - *n_acquisitions* is $64 \times n_frame$ (compared to nominal mode)
- *suffix*: 3-columns array containing the time in SCET coded on 3 unsigned integers. One can convert into a real double precision value with the IDL routine *v_scet(s0, s1, s2)*.
- *table*: 3-columns array containing, for each channel:
 - The wavelength, in micron
 - The spectral full width at half maximum (FWHM), in micron
 - This column should contain the $1-\sigma$ error on the radiance, but it's currently not computed. This column is filled either with the error code -999.999 or with 0.0.

7.1.5 Internal calibration sequences

Internal calibrations produce a backup qube and a set of two spectra (see §6.3.3). Relevant fields are those of raw qubes. Dimensions of the field '*qube*' are always $432 \times 256 \times 7$, that is to say seven 2D images of 432×256 pixels. The two spectra are stored in a separated file.

7.2 Acquisition sequences

7.2.1 Observations and darks patterns

One telecommand (TC) sent to Virtis-H leads to one session of acquisitions. Observations and dark acquisitions are interleaved, following this pattern:

1 dark

h_dark_rate x 1 observations

1 dark

...

Where *h_dark_rate* is specified at the TC stage.

In order to reduce the data volume, Virtis-H can sum acquisitions onboard. The parameters *h_sum = yes* and *h_n_sum_frame = n* lead to sum *n* acquisitions.

Another way to reduce data volume is to use the parameter *h_n_frame = p*. In this case, only 1 acquisition among "*p*" is sent.

Usages of *h_n_sum_frame* and *h_n_frame* are mutually exclusive.



This covers the usual observation modes. Details of H observing modes are provided in [RD1].

7.2.2 Acquisition_id

Each acquisition has its own *acquisition_id* during a session, which is stored in the associated housekeeping parameters. The first acquisition (which is always a dark) has the number 1. The following $h_dark_rate \times I$ observations have the numbers 2 to ($h_dark_rate + I$).

In nominal mode, the reported *acquisition_id* is the one of the last spectrum of the current 64-spectra packet. Then all the 64 spectra of the same frame have the *acquisition_id* of the last one.

Dark current measurements are sent independently each time they are acquired. Thus each dark has its own *acquisition_id* reported in the housekeepings.

In backup mode, each frame is sent with its own *acquisition_id*.

7.3 Filenaming convention

All data product files throughout different VIRTIS data sets are named using the same file naming convention [RD4]. Data qubes are named according to the suffix indicating the channel, the spacecraft clock reset number and the acquisition SC_CLOCK_START_COUNT (integer part). The possible suffix values are related to the data transfer mode:

- H: H image transfer mode (backup observation mode)
- S: H single spectrum transfer mode (including dark current files in nominal mode)
- T: H "64-spectra frame" transfer mode (nominal mode)

For example, acquisitions starting at SPACECRAFT_CLOCK_START_COUNT = 1/0432992043.44607 (1/ is the clock reset number) are named: *T1_00432992529.QUB* for a nominal spectrum

The extension of raw files is *.QUB*

The extension of calibrated qubes is *.CAL*

Interpolated dark acquisitions are stored in files with extension *.DRK*



8 Radiometric Calibration

8.1 Calibration process

The calibration process follows several steps described in the flow diagram hereafter (Figure 1). We will describe those steps in details.

8.1.1 Nominal and Backup modes

As said in §6.3 the raw data are acquired in two modes: Nominal and Backup. In Nominal mode, the data are stored in spectrum format. In Backup mode, the data are stored as 2D images. For these data, we first need to transform the collection of 2d images into a collection of spectra. We compute for each channel of each order the mean of the 5 pixels around the relevant position given by the pixel map. All 432-channels orders are concatenated, beginning with order 0. The resulting 3456 elements array is returned (same format as the Nominal spectra).

For data from tests at sub-system level, the pixel map is applied starting from position $[xwin, ywin]$ of the detector.

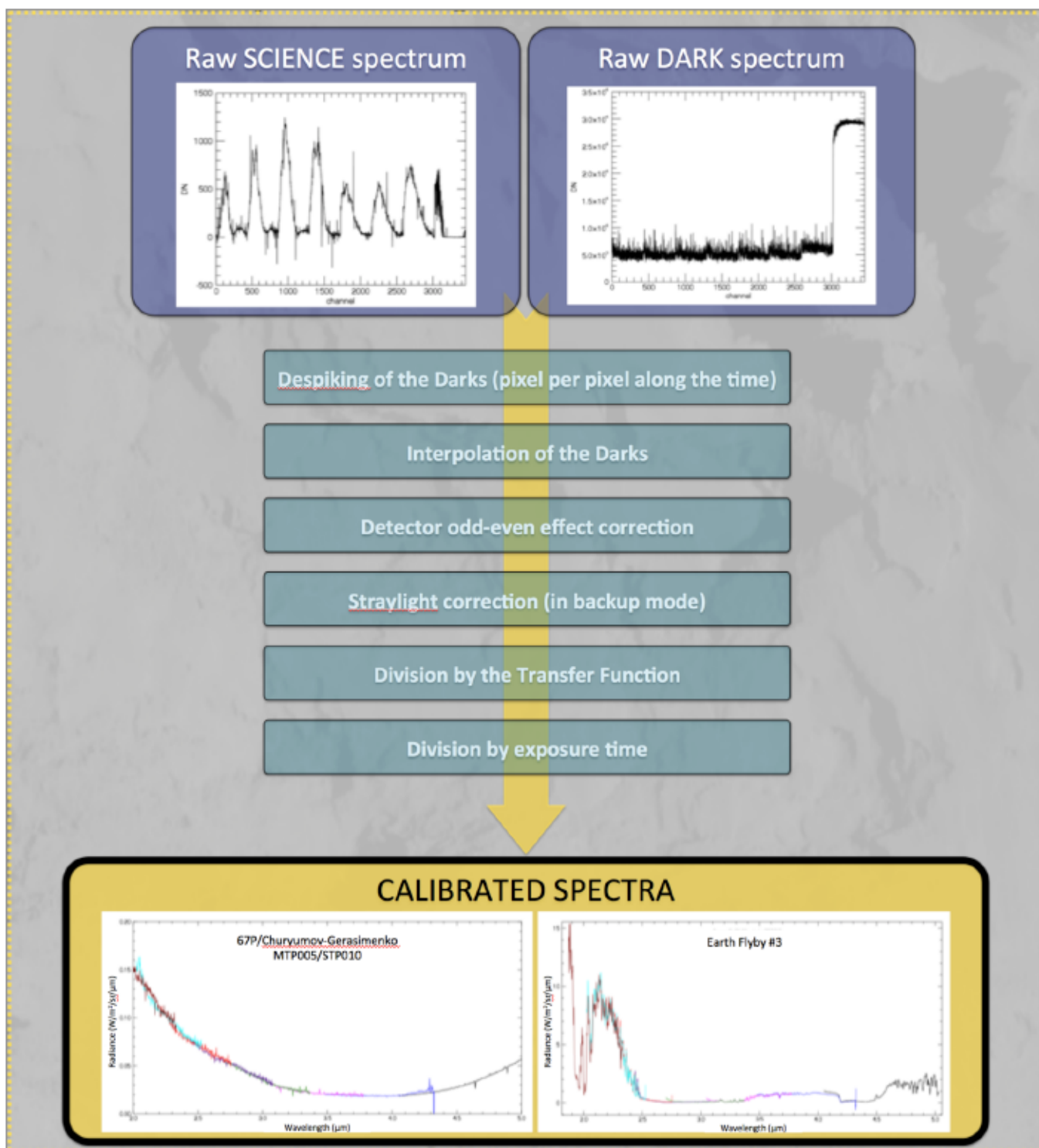


Figure 1: Flow diagram describing the calibration process for Nominal data



8.1.2 Despiking and interpolation of dark spectra

Due to cosmic particles, which sometimes go through the detector, some erratic values (spikes) are detected in the data. In a first step, we need to despik the dark spectra. We perform the despiking channel by channel along the time dimension in the dark measurement sequence. For each channel considered we perform a filter at 3 sigma to eliminate the spikes.

The first step of the calibration is to recover an optimized dark spectrum. In Nominal acquisition mode, the latest dark acquired at the end of a frame (64 spectra) is subtracted on board from the frame's spectra (cf. §7.1). First, we re-add the subtracted dark to the frame's spectra. Then, we interpolate the despiked dark measurements acquired between the beginning and the end of a frame to obtain one dark per spectrum. Finally, we subtract the interpolated darks to the frame's spectra. This compensates dark current variations related to possible changes in temperature.

Note that for the Backup mode data, we re-add the dark image to the science images before extracting the spectra as described in §8.1.1. Dark measurements are identified from the housekeeping parameters and processed separately (we use the same method to extract dark spectra from the dark images). Then we proceed as explained above for the interpolation.

8.1.3 Detector odd-even effect correction

The second step of the calibration process consists in correcting the odd-even effect due to different responses of even and odd columns of the detector (Fig. 10). We separate odd and even pixels; we interpolate the 216 even pixels responses over a 432 points vector. Idem for the odd channels. The corrected dark is the mean of these two vectors.

8.1.4 Stray light correction

The third step of the calibration process consists in correcting the stray light effect. We currently apply this correction to the Backup data only, because the stray light contamination is directly observed only in the 2D images of the detector (correction described in §10.1.1.2). This information is lost in spectrum format, therefore cubes acquired in nominal mode are not currently corrected (see §8.2.1).

8.1.5 Division by transfer function and exposure time

To obtain the calibrated spectra, we need to divide the spectra by the transfer function of the instrument. The current transfer function is derived from a physical modeling of Lutetia based on the observations: a first order calibration derived from ground measurements is used to get the radiance spectrum of a selected area on Lutetia; spectral reflectance and thermal emission are fit on this spectrum; the ratio of the model to the



measurement provides the transfer function (the detailed procedure is described in §10.1). This two-step process provides a transfer function free from features of remaining water vapor and CO₂ in the ground calibration tank, which would affect the detection of molecular species in the coma in spite of a tentative removal (§10.1.1.3).

Finally we also divide the spectra by the exposure time of the acquisition (available in the PDS label) to obtain the calibrated spectra in radiance, with unit W/m²/sr/μm.

Absolute radiance levels are controlled by the ground-based measurements, and are estimated to be accurate to ~20-30%.

8.1.6 Conversion to reflectance

Surface spectra are more commonly studied on a reflectance scale. The solar spectrum used in such conversions by the VIRTIS team is the high-resolution Kurucz (1997) spectrum convolved with the instrument response function derived in section 9.

8.2 Open issues on the calibration

Some channels behave erratically after calibration, and this varies from session to session. No filtering is applied to preserve possible narrow emission/absorption features. Inconsistencies in level can be noticed in particular at the extremities of the each spectral order where the transmission is low, and where dark current variations and stray light can contribute significantly.

8.2.1 Stray light correction in nominal mode

In backup mode, stray light is directly observed as a bright patch between spectral orders on the detector (Fig. 12). This implies that it is due to non-dispersed light reaching the detector in some conditions. Signal analysis suggests it is due to a reflection in the entrance optics, and that its intensity depends on the location of light sources around the nominal Field of View. The bright patch overlaps the short wavelength side of all spectral orders, where it contributes to the output signal – especially in order 0 where the long wavelength flux is not filtered. In backup mode, interpolation of the bright patch between spectral orders is currently used to remove most of this contribution (Fig. 12b). In nominal mode though, a correction has to be derived from the spectrum itself. Such a correction is currently under study and will be implemented in a future version of the archive.

A typical stray light pattern in spectra of the comet is displayed in Fig. 2a for reference. As a general rule, long wavelength extremities of spectral orders are not affected by this contribution and are more reliable (although the signal to noise ratio also decreases rapidly at both ends of the spectral orders). However, this pattern displays only low frequency variations. Therefore, short wavelength extremities of spectral orders can be used to study high-resolution signatures from the coma in a relatively narrow range, provided that a local continuum is fit on individual spectra.

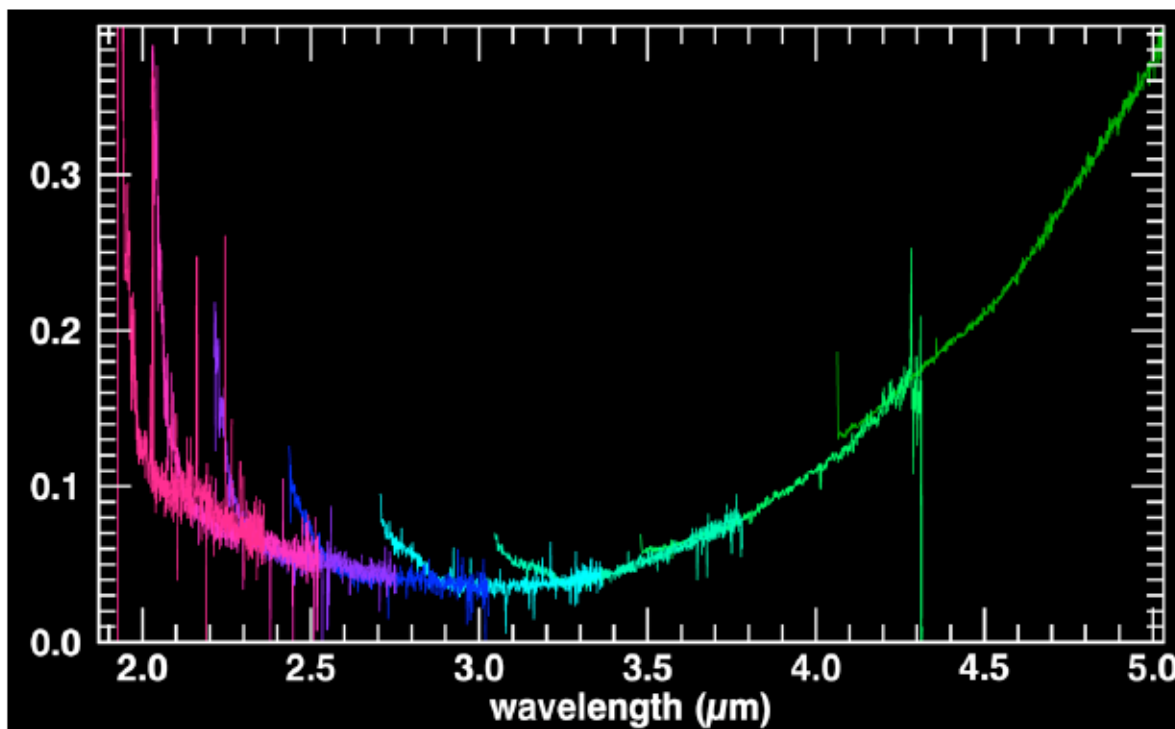


Figure 2a: Example of radiance spectrum of the comet affected by stray light. Excess signal on the short wavelength side of each order is typical from the stray light pattern. The high frequency variations are partly due to the odd/even effect and can be processed.

8.2.2 Improvement of odd/even effect correction

A refinement of the odd/even correction is under study and will be included in a future version of the archive.

8.2.3 Strabismus

VIRTIS-H actually uses two gratings with different blaze angle, so as to enlarge the useful range in each spectral order. These two gratings do not see exactly the same part of the slit, and therefore do not have exactly the same Field of View. Whenever high frequency structures exist (e.g., shadowed areas on the nucleus), the signals from the two gratings do not fully match. This effect is not accounted for in the present version of the calibration, and spectra acquired near illumination boundaries are affected by a visible artifact. This is essentially negligible in the coma.

This effect is being studied, and a partial correction will be included in a future version of the archive.



8.2.4 Signal to Noise estimate

The signal to noise ratio is difficult to compute in the presence of systematic errors related to stray light added in some situations. For this reason, detailed noise estimates are not currently included in individual calibrated files (a placeholder is filled with value 0.0 or -999., see 7.1.4). A provisional 1-sigma estimate is derived from statistics of measurements in a typical observation of 67P nucleus, when the comet is still warm and significant level is measured at long wavelengths (Fig. 2b and 2c). Because stray light is actually detected in this session, this estimate may be biased in the short wavelength side of each spectral order and must be used with caution.

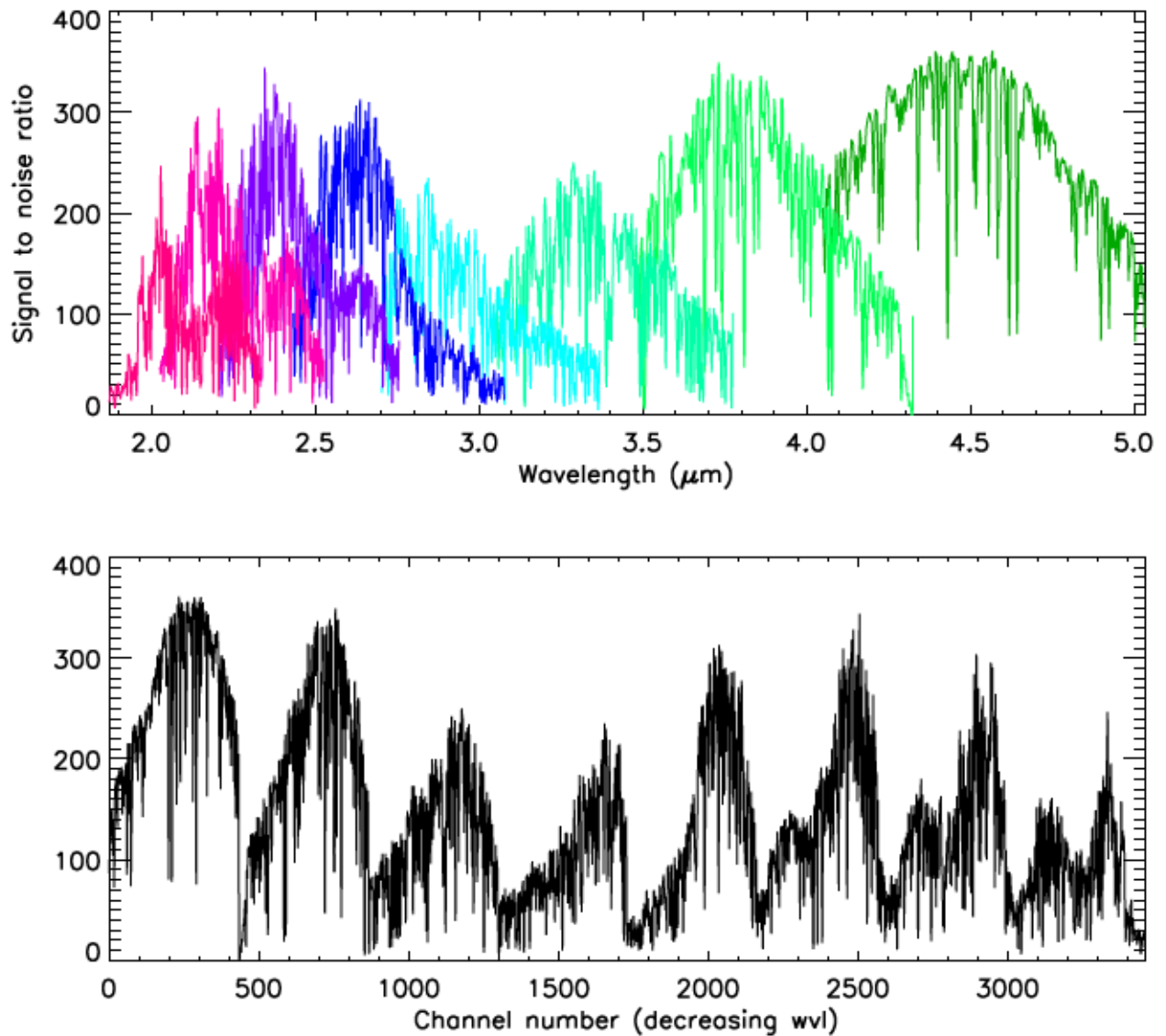


Figure 2b and 2c: 1-sigma SNR derived from session T1_00418835363 in STP103.
 2b: against wavelength, with grating order overlaps; 2c: against channel number (~ decreasing order and wavelength)



9 Spectral calibration

9.1 Principle

The spectral calibration consists in determining the central wavelength of each channel.

The internal spectral calibration is made by mean of a pre-calibrated Fabry-Perot with respect to the temperature. The Fabry-Perot emission (Figure 3) gives between 20 and 10 lines depending of the grating order. This device allows finding back the spectral registration of the instrument. The absolute position of each known spectral lines on the detector is gauss fitted for each order and used to reconstruct the spectral registration of the instrument, which fits a 2-degree polynomial function.

Those polynomial functions are then used to give for each channel the correspondence between the channel number and the wavelength.

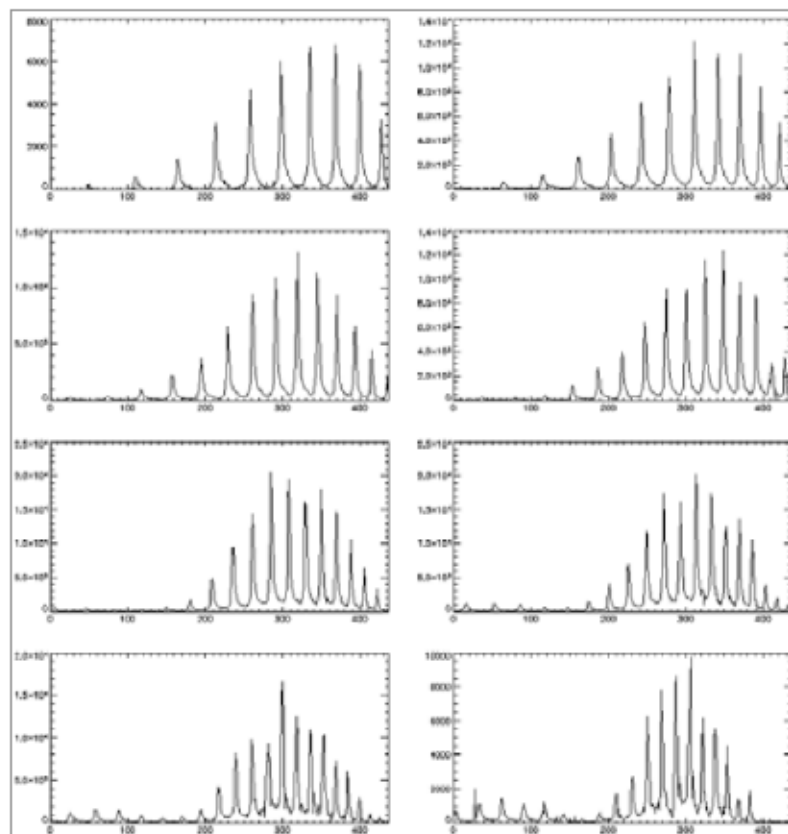


Figure 3: Emission of the Fabry-Perot spectral lines in each order



9.2 The PxLMapL

The PxLMapL is a table of 3 coefficients per order. Those coefficients are the coefficients of the 2-degree polynomial function giving the correspondence between the channel number and the wavelengths.

For each order, we scan the spectrum to find the FP spectral line having a level upper than 'Offset' using a gauss fit function. The peak positions returned by the Gaussian fit function of each spectral line are stored in a table.

Using the FP temperature 'dT' and the initial room temperature FP thickness 'e', a table of theoretical wavelengths emitted through the FP is generated.

For each order a table 'lambdamin' of first expected wavelengths at the border of the detector is determined. The maximum error tolerated is given by the difference between two consecutive FP spectral lines. If the table is false, the registration will be false by a factor that is the difference between two consecutive FP spectral lines. Nonetheless, the error will be identified immediately on a science spectrum. If so the 'lambdamin' table has to be readjusted.

Once the table of FP wavelengths and positions on the detector are created for each order, the 2-degree polynomial fit is used to generate the coefficients. Those coefficients are then stored in a PxLMapL file. The wavelength vectors are stored in the calibrated files.

9.3 Accuracy of the spectral calibration process

The sources of errors to construct the registration table are:

- The accuracy of the gauss fit for each FP spectral line;
- The deviation from a 2 degree polynomial function for the registration;
- The initial room temperature thickness for the FP.

The addition of all the errors gives a maximum estimated global error for the registration of 1 channel.

Figure 4 and Figure 5 display the maximum drift of the registration in spatial and spectral directions as a function of spectrometer and detector temperatures, using all the internal calibrations since the Steins Flyby (Sept. 2009). In the spatial direction (Y dimension of the detector) the maximum drift is estimated to 0.09 pixel; in the spectral direction (X dimension of the detector), the maximum drift is estimated to 0.41 pixel.

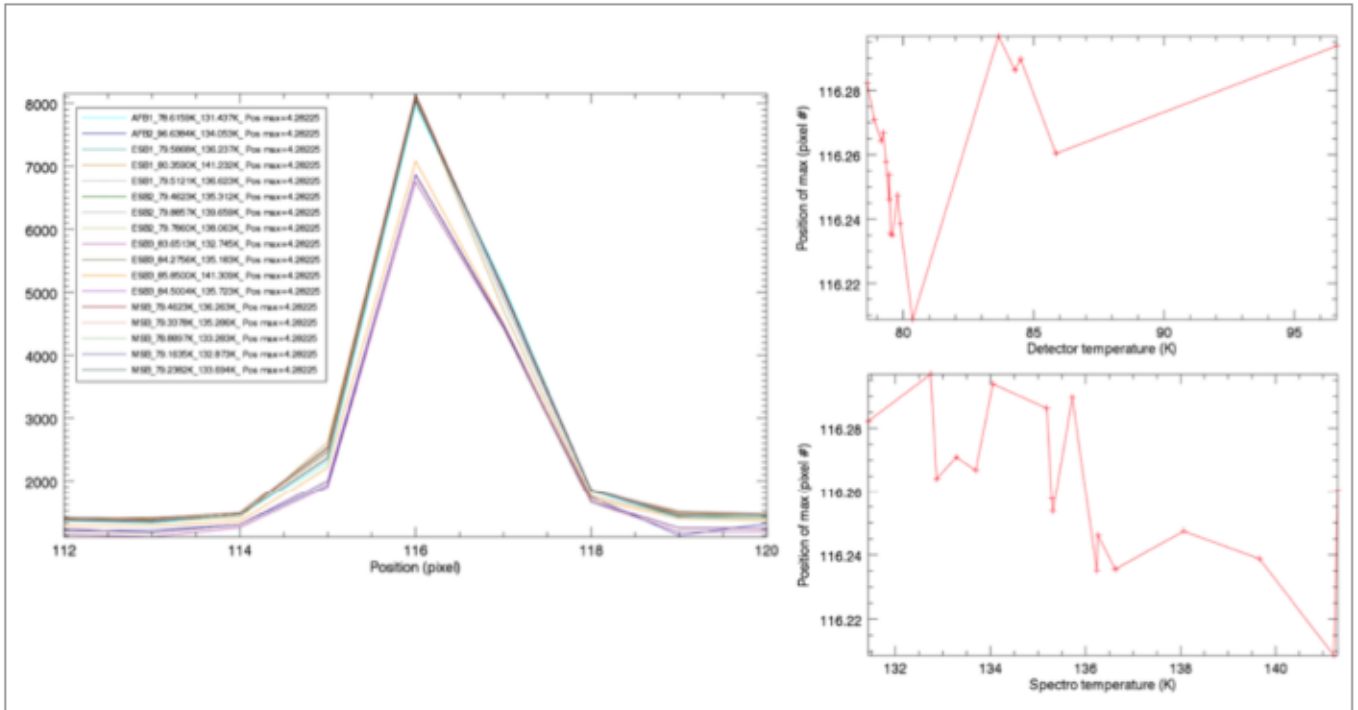


Figure 4: Registration drift estimation in spatial direction using all internal calibrations since Steins Flyby

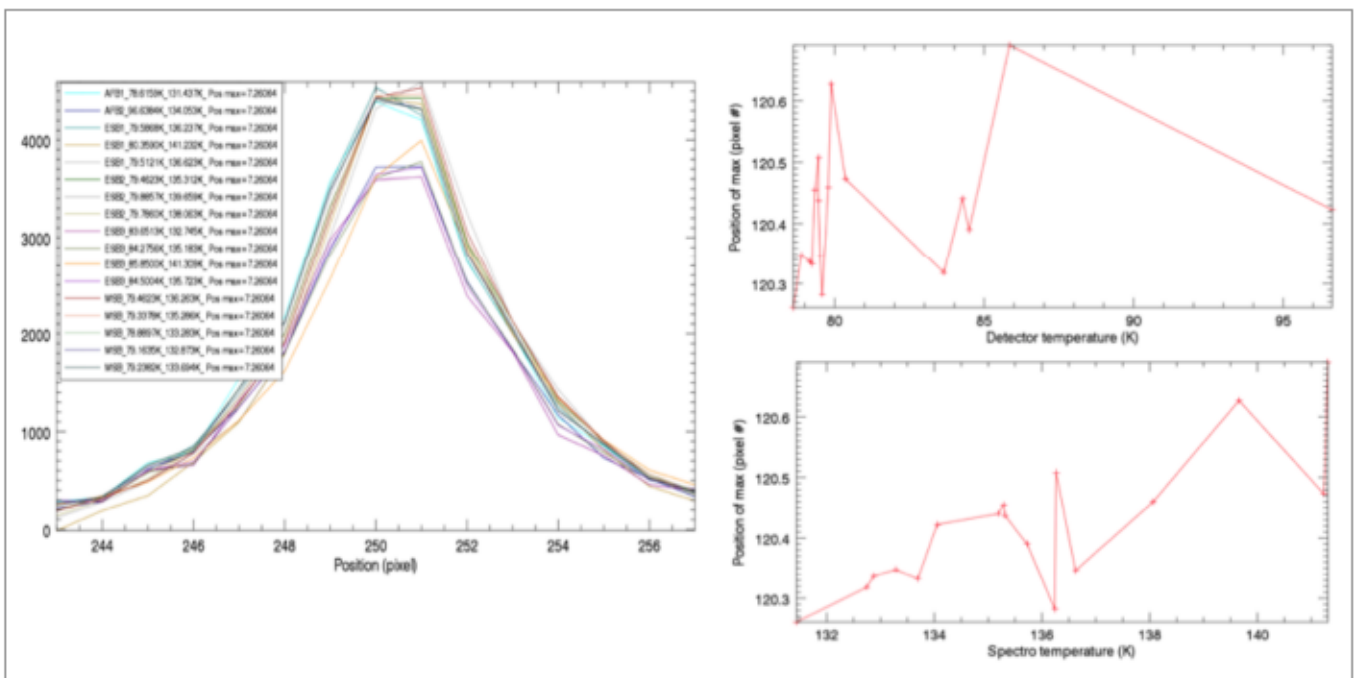


Figure 5: Registration drift estimation in spectral direction using all internal calibrations since Steins Flyby



These errors can be decreased by using science spectra having well known spectral lines and by adjusting the parameters of the function. We have done this to improve the spectral calibration in orders 0-2 and 4 using data from the Earth and Mars flybys, and from the Escort Phase data of comet 67P/Churyumov-Gerasimenko (MTP019/STP070) based on theoretical modeling of those lines (see example on Figure 6). This results in particular in a much better match of overlapping orders.

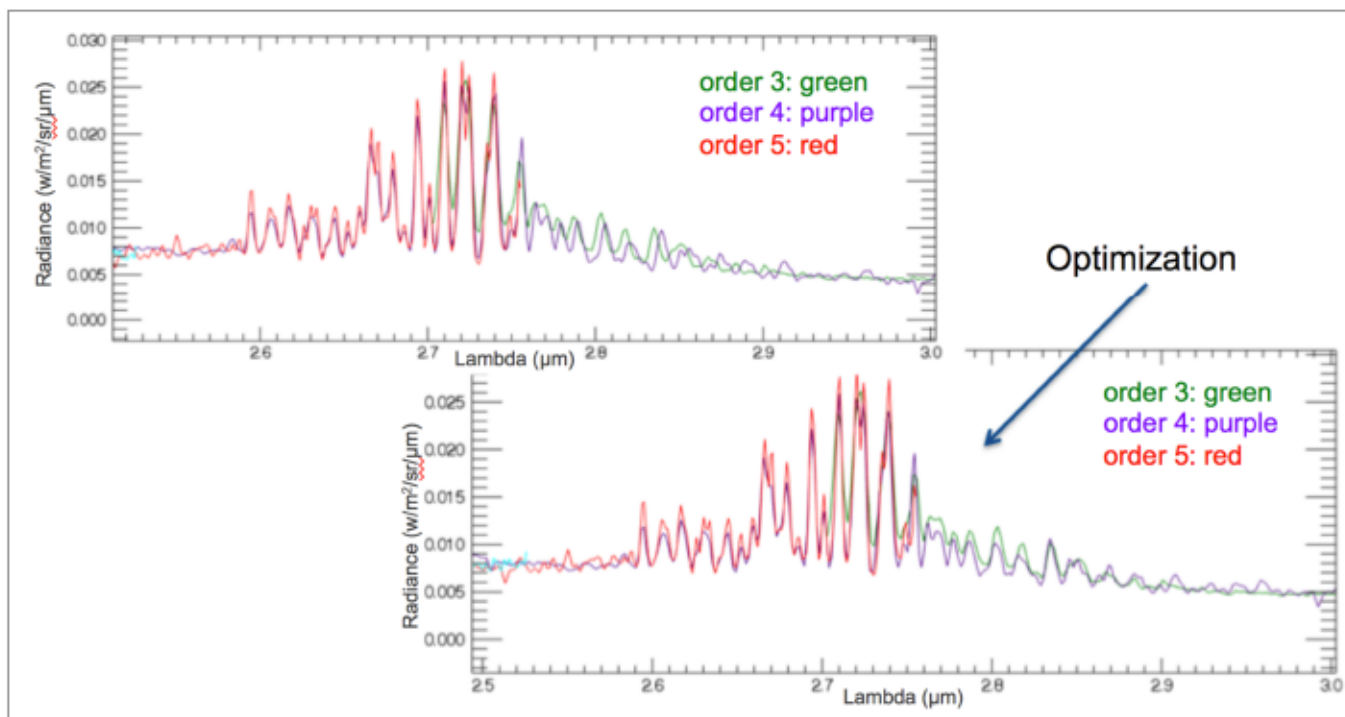


Figure 6: Optimization of the spectral registration in order 4, using ESCORT phase data and theoretical model

9.4 Channels spectral profiles

9.4.1 Definition

The spectral registration given by the PixelMapL table does not take into account the spectral profile within the image of the slit. This profile is the spectral response of the instrument.

Owing to the optical design, the spectral response varies significantly along the spectrum. No dedicated on-ground calibration was able to measure this spectral response. Nonetheless, as VIRTIS-H is almost diffraction limited, this profile can be estimated by the diffraction theory using the optical parameters of the spectrometer.



9.4.2 Spectral profile calculation

The spectral response is calculated for each wavelength in each order using the diffraction theory.

It is the convolution of the diffraction profile by the width of the slit image. The formula used to calculate the spectral response are given below:

Max. intensity	$\beta(\lambda, k) = \arcsin(k \times n \times \lambda - \sin(\alpha))$
Resolution per pixel	$\Delta\lambda(\lambda, k) = \frac{-\cos(\beta(\lambda, k))}{n \times k} \times \frac{pxl}{f}$
Energy profile due to diffraction by grating	$I(x, \lambda, k) = \text{sinc}\left(\pi \times \frac{L \times \cos(\beta(\lambda, k))}{\lambda} \times \arctan\left(\frac{x}{f}\right)\right)^2$
Window function	$\Pi(x, a) = \begin{cases} 1 & \text{if } x < \frac{a}{2} \\ 0 & \text{otherwise} \end{cases}$
Convolution of the energy a λ by a pixel	$Ic(x, \lambda, k) = \int_{-0.1\text{mm}}^{0.1\text{mm}} I(x-t, \lambda, k) \times \Pi(t, pxl) dt$

With:

- λ is the wavelength
- k is the order number
- α is the incident angle on the grating
- n is the groove density of the grating
- pxl is the pixel size
- L is the width of the grating
- f is the objective focal length

The following Figure 7, Figure 8 and Figure 9 show the spectral response at two different wavelengths in two different orders. The blue line shows the geometrical slit width.

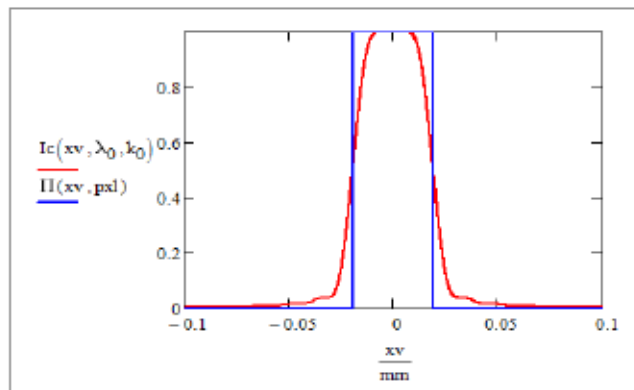


Figure 7: Spectral response @2 μm , order 7

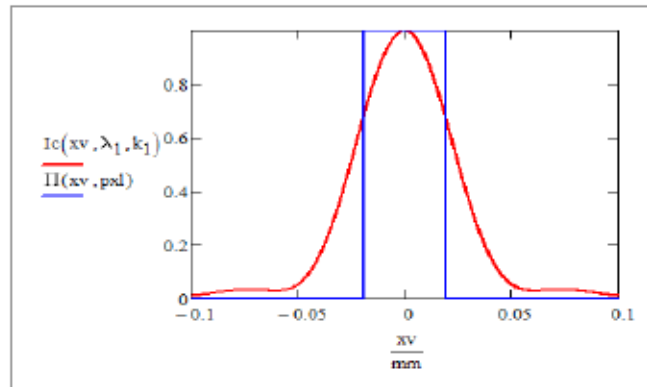


Figure 8: Spectral response @5 μ m, order 0

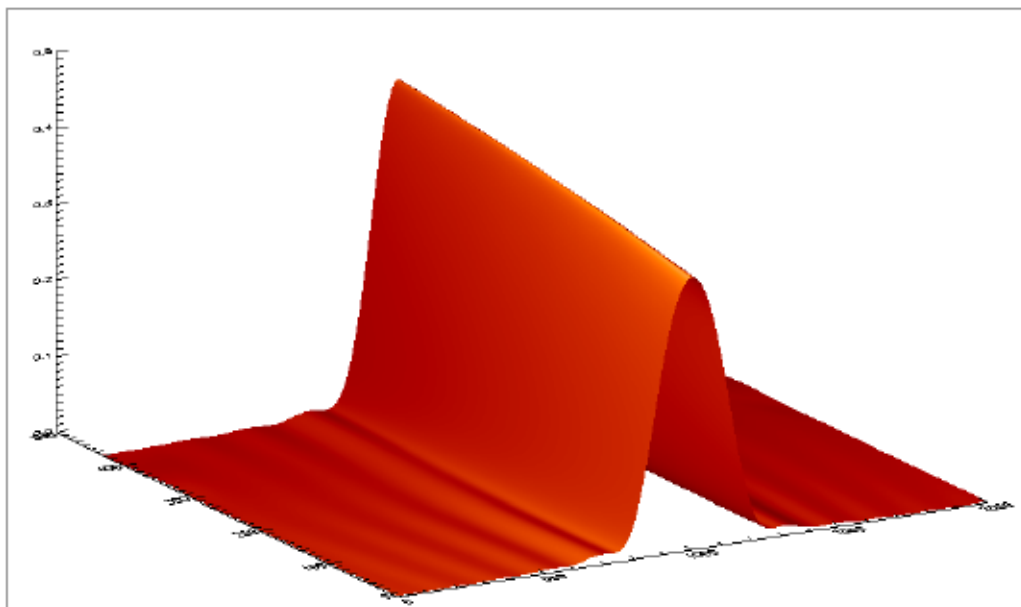


Figure 9: Plot of the spectral profile through order 0



10 Annexes

10.1 Derivation of the transfer function

To recover the calibrated spectra from raw data, a transfer function (TF) is used. The transfer function is usually computed from measurements done during the ground calibration phase. In our case, due to various problems with the on-ground calibration data (traces of H₂O and CO₂ in the vacuum chamber, odd-even effect...) and due to variations observed after launch and the lack of calibration during the Cruise Phase, we followed a new approach and defined a new method to compute the TF. This method is composed of two steps described below.

10.1.1 STEP 1: ground-based calibration

The first step consists in building a first "BETA" transfer function, using on-ground calibration blackbodies data as input. As said previously, those data contains some flaws that we need to correct first: odd / even effect, stray light, H₂O and CO₂ contaminations.

10.1.1.1 Odd/even effect correction

This effect is due to a difference of gain and offset between the output voltage of the odd and even columns of the detector. It is only present in the X direction of the matrix (cf. Figure 10) It depends of the charge (ADU) and decreases with the charge (non-linear effect). We use detector calibration measurements performed at LESIA on the YACADIRE test bench to correct this effect.

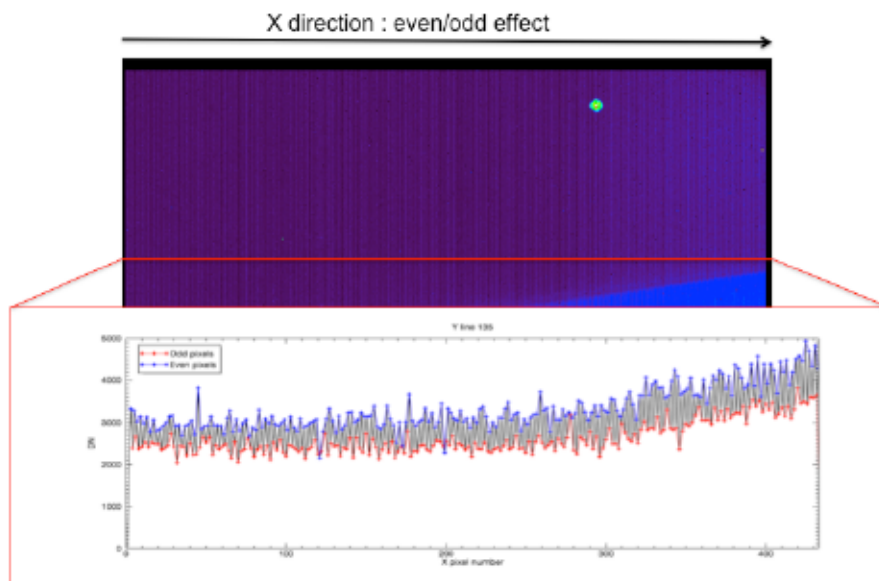


Figure 10: Odd/even effect on the Virtis-H matrix detector (Up: Backup image, Down: extraction of a pixel values in X direction)

In Figure 11, an example of the correction curves we obtain using YACADIRE data. We interpolated those curves to obtain correction factors that we apply on odd channels of raw data.

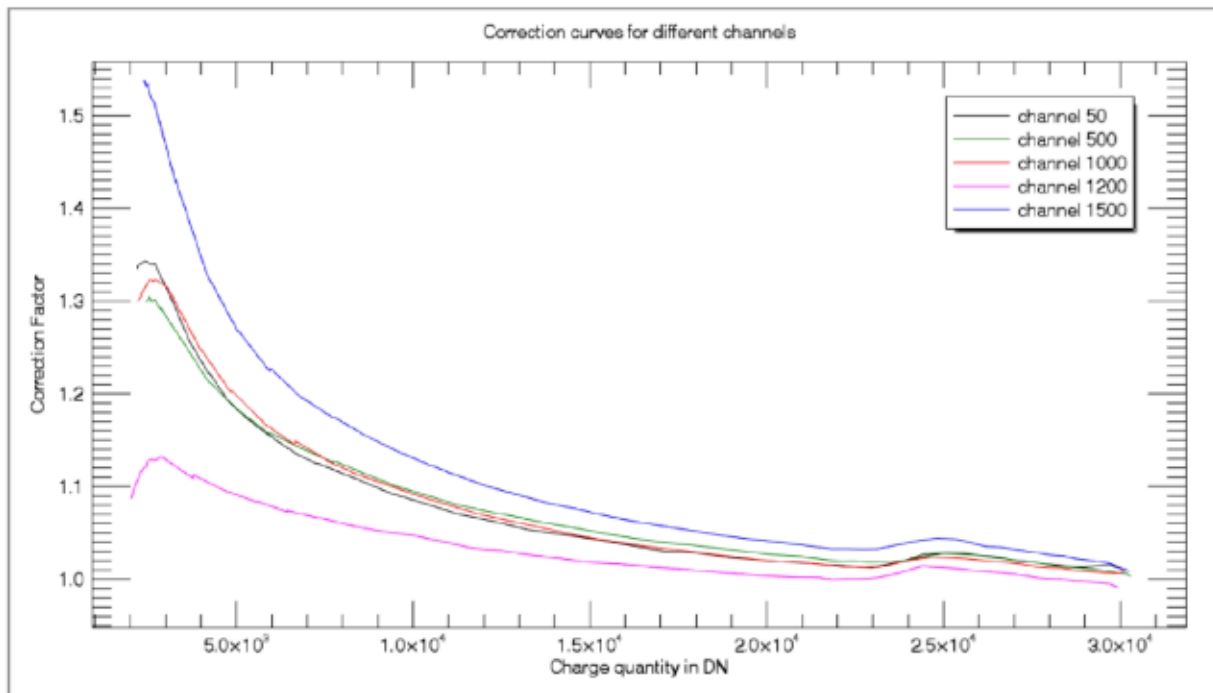


Figure 11: odd/even correction curve derived from YACADIRE measurements

10.1.1.2 Stray light correction

Stray light is present in all on-ground data. This effect is polluting the right bottom corner of the detector matrix by adding dirty flux to the useful signal (cf. Figure 12). This effect can be 2D-fitted to obtain a map of the stray light. Thus we subtract this map from the 2D-raw images to correct this effect on data acquired in backup mode.

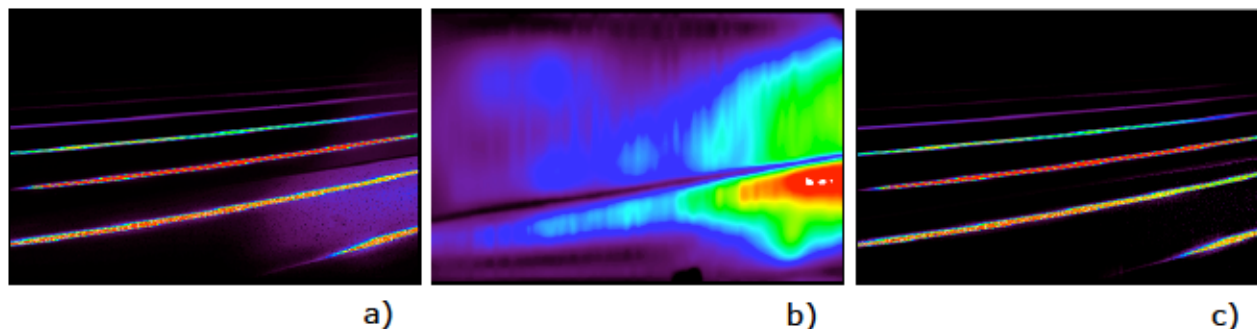


Figure 12: a) Backup raw image (2D) - b) map of the stray light - c) Backup raw image corrected from the stray light effect



10.1.1.3 Correction of H₂O and CO₂ contamination

During on-ground calibration, blackbody stimuli bench and setup are placed under nitrogen environment whereas VIRTIS instrument is placed in vacuum chamber. A small quantity of H₂O and C₂O vapor remains. This leads to the detection of H₂O and CO₂ transmission spectral lines in the calibration blackbodies data. To remove those spectral lines, a simple low frequency filter is not sufficient, as it will distort the transfer function. We use the HITRAN¹ database, adjust the molecules concentration and convolve by the VIRTIS-H instrument profile. We optimize the correlation coefficient between measurement and model by adjusting the molecule concentration. In Figure 13, an example of HITRAN database fitting to correct H₂O transmission lines.

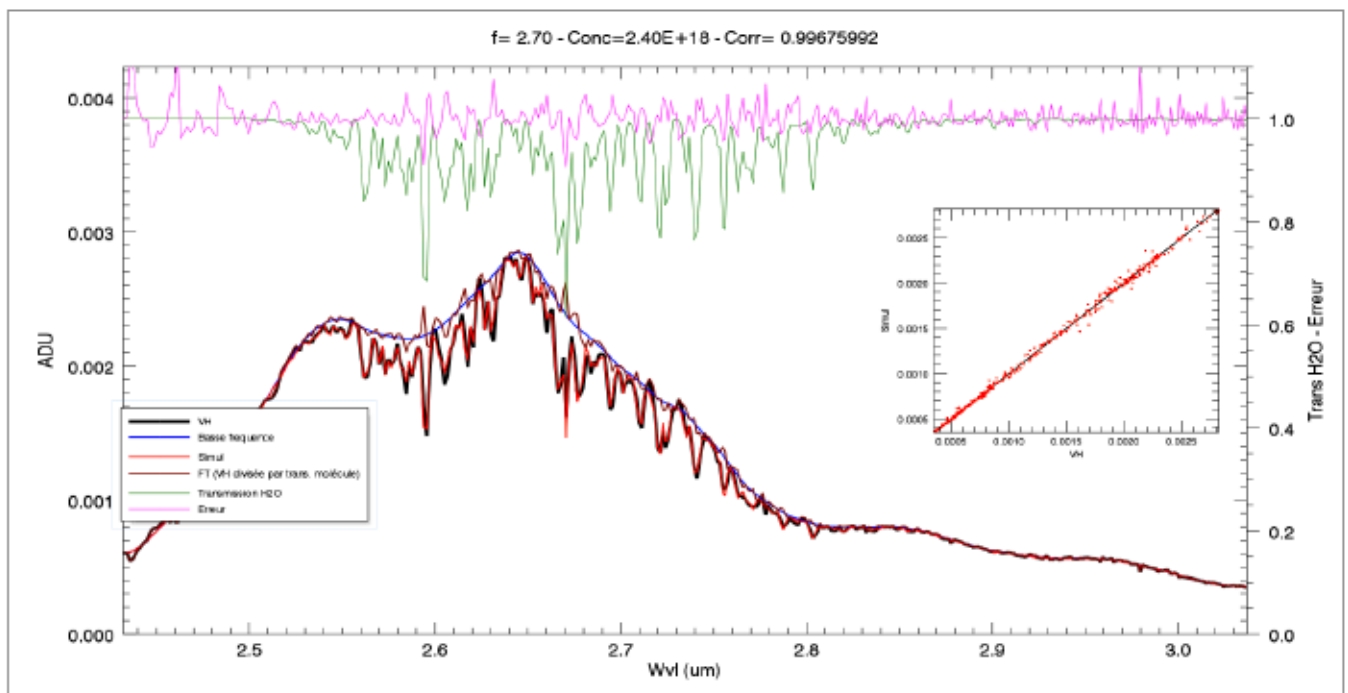


Figure 13: H₂O vapor correction using HITRAN. Black: measurement. Green: modeled gas transmission. Dark red: refined TF. Pink: final residuals.

10.1.1.4 Creation of a beta transfer function

After applying all the corrections described above to the on-ground blackbody calibration data, the final step to create the BETA transfer function consists in adjusting the

¹ <http://hitran.org>



radiometric level by fitting calibration black bodies. The complete procedure of the ground-based calibration is described in the flow diagram below (Figure 14).

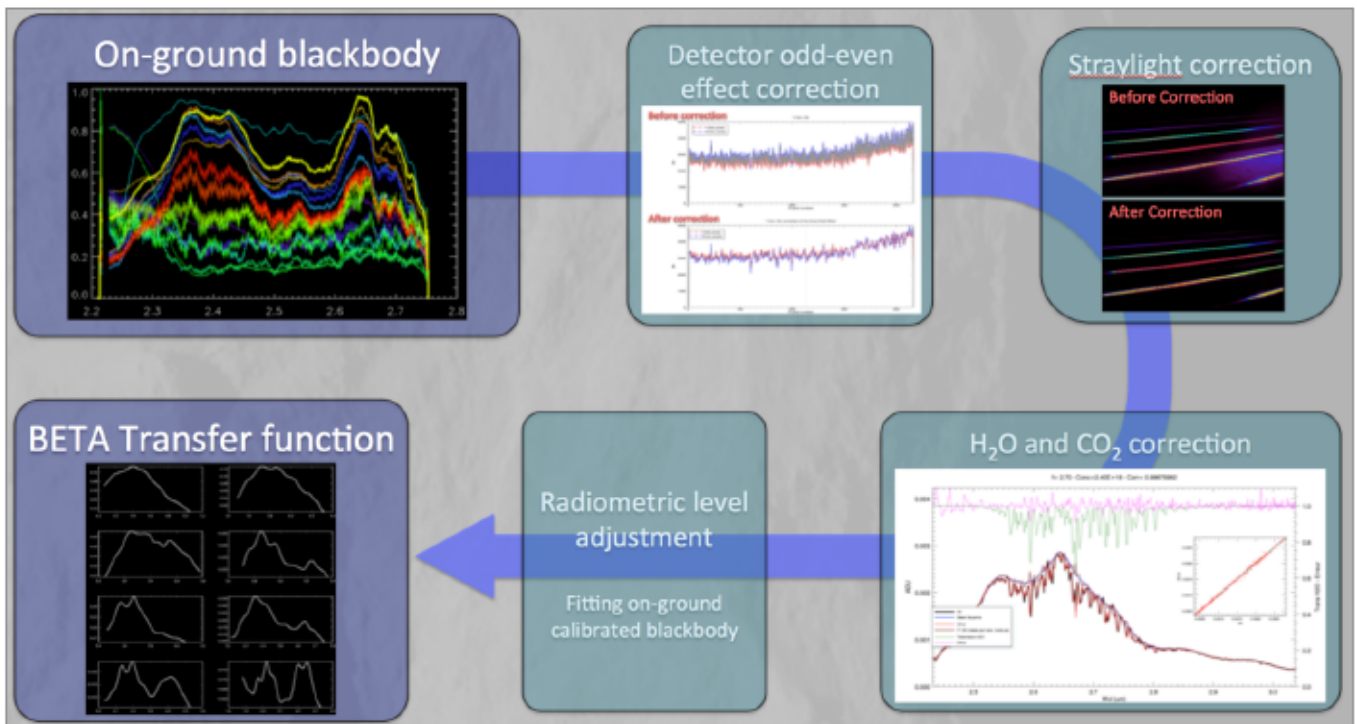


Figure 14: Flow diagram of the BETA Transfer Function creation

10.1.2 STEP 2: Lutetia as a calibrator

The transfer function derived from ground measurements proved to be inconsistent when applied to flight data, which was ascribed to small shifts between optical parts occurred during the launch with Ariane 5. Besides, the remaining gas absorptions in the calibration tank are difficult to remove at a level not perturbing the measurements in the coma. Finally, no point source could be targeted during cruise with a single-pixel instrument and provide enough flux to derive a new calibration.

The second step of the transfer function derivation therefore consists in using the asteroid Lutetia observed during Cruise Phase as a calibrator. The process is described in the flow diagram below (Figure 15). A selected area on Lutetia is integrated to provide a "Reference spectrum", both in raw data and calibrated with the above procedure. The radiance reference spectrum of Lutetia is modeled as the sum of reflected and emitted light. The ratio of the Raw Lutetia spectrum and the model provide the Final Transfer Function used on flight data.

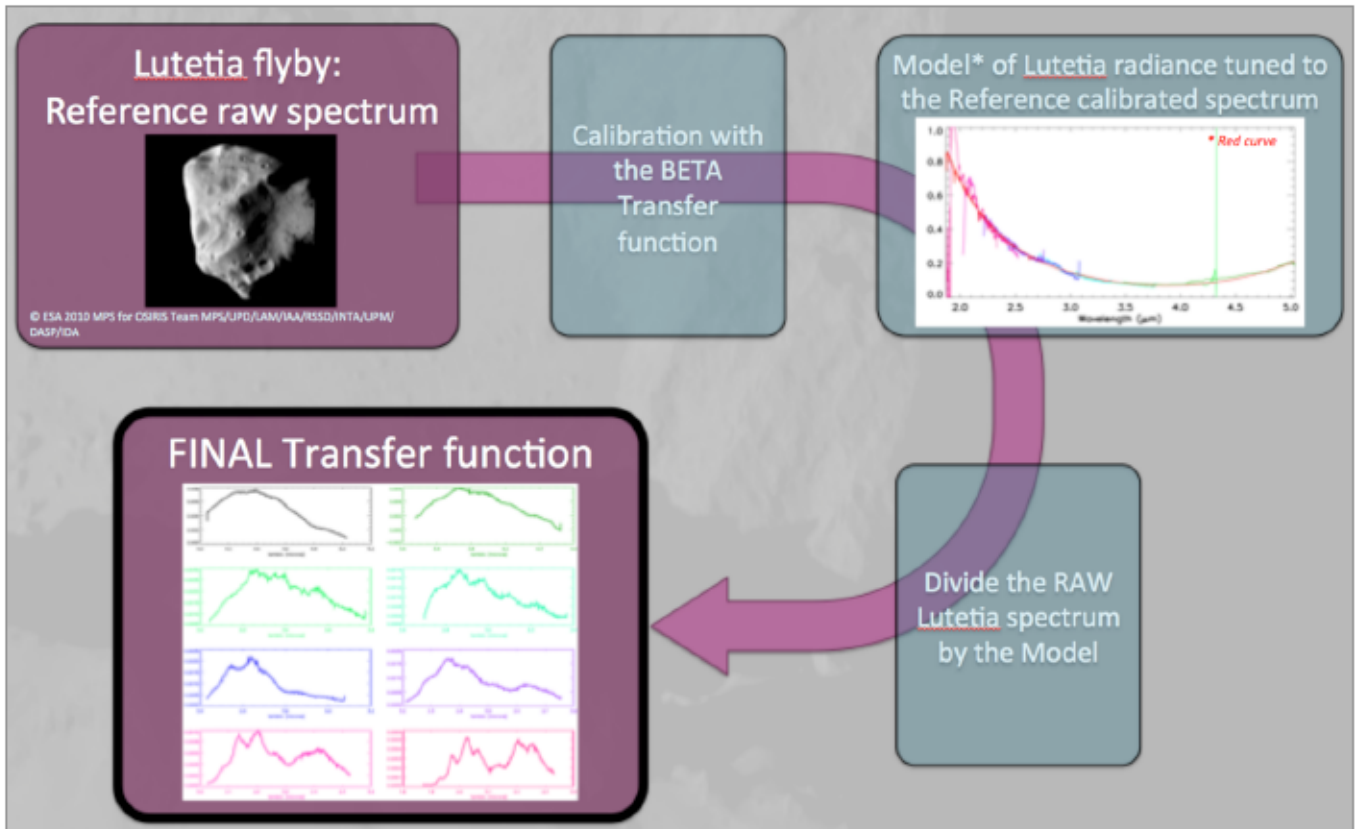


Figure 15: Flow diagram of the Final Transfer Function creation

10.2 Corrupted darks

10.2.1 Description of the problem

A serious problem was identified in 2006 on the model of VIRTIS-H flown on Venus-Express: some dark current acquisitions contained science signal. After investigation, this appeared to be due to an incorrect synchronization of the shutter in the onboard software, and the same problem affected the Rosetta software (see RD3).

Figure 16 shows an example: the shutter opens during dark current acquisition (dotted line). A growing fraction of the exposure is performed with the shutter open, until it cycles from the start; the solid line represents a correctly interpolated dark current, which in this case decreases with instrument temperature.

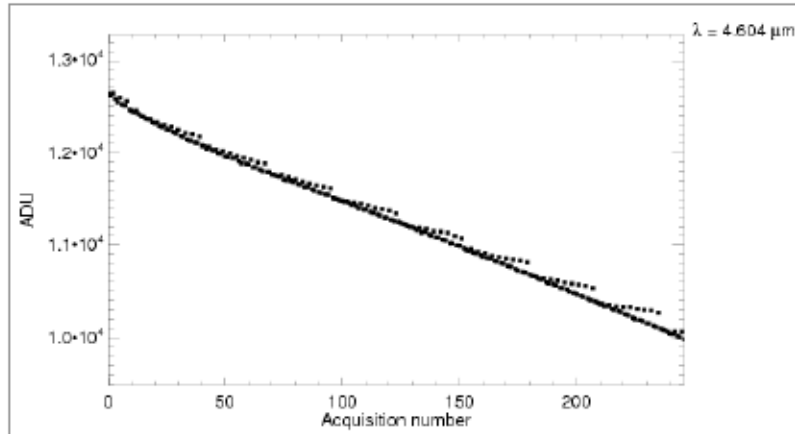


Figure 16: Example of dark corruption

10.2.2 Workaround

It is of course impossible to remove a science signal mixed in the dark current. The only solution is to identify the corrupted dark acquisitions and to skip them during data processing. Because this identification process is partly automatic, some corrupted darks may be still present.

The onboard software has been modified and uploaded onto the spacecraft on the 27th of August 2009 (before the Steins flyby), which fixed the issue permanently. Only pre-Steins observations are therefore affected by this issue. The problem is addressed, but results in a reduced number of dark current measurements and therefore reduced signal-to-noise ratio. Since the targets are very bright (Mars and first 2 Earth swing-by), this is a limited issue in most cases.



Table of Illustrations

Figure 1: Flow diagram describing the calibration process for Nominal data12

Figure 2a: Example of radiance spectrum of the comet affected by stray light.....15

Figure 2b/c: Signal to noise estimate.....12

Figure 3: Emission of the Fabry-Perot spectral lines in each order.....17

Figure 4: Registration drift estimation in spatial direction using all internal calibrations since Steins Flyby.....19

Figure 5: Registration drift estimation in spectral direction using all internal calibrations since Steins Flyby.....19

Figure 6: Optimization of the spectral registration in order 4, using ESCORT phase data and theoretical model20

Figure 7: Spectral response @2 μ m, order 7.....21

Figure 8: Spectral response @5 μ m, order 0.....22

Figure 9: Plot of the spectral profile through order 0.....22

Figure 10: Odd/even effect on the Virtis-H matrix detector (Up: Backup image, Down: extraction of a pixel line values in X direction).....23

Figure 11: Odd/even correction curve from YACADIRE24

Figure 12: a) Backup raw image (2D) - b) map of the straylight - c) Backup raw image corrected from the straylight effect.....24

Figure 13: H2O vapor correction by HITRAN database fitting.....25

Figure 14: Flow diagram of the BETA Transfer Function creation.....26

Figure 15: Flow diagram of the Final Transfer Function creation27

Figure 16: Example of dark corruption28